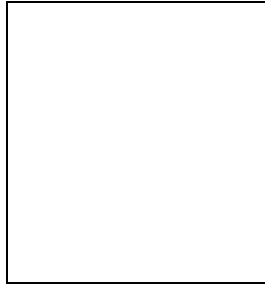


CLUSTER SURVEYS

Isabella M. GIOIA

Istituto di Radioastronomia del CNR, Bologna, Italy
Institute for Astronomy, Honolulu, Hawai'i, USA



I review some of the current efforts to create unbiased samples of galaxy clusters. Readers are referred elsewhere for general wide area sky surveys and redshift surveys, and for Sunyaev-Zeldovich, radio, infrared and submm surveys, some of which were not designed to search primarily for clusters. My focus will be on optical and X-ray samples and on high redshift clusters.

1 Importance of Galaxy Clusters

Clusters of galaxies are the largest virialized, bound systems known. Their study yields a wealth of information on structure in the Universe over a large range of length scales and on the evolution of that structure over a long time span. Individual clusters are the ideal laboratory for multiwavelength studies of many physical processes involving various constituents of the Universe (galaxies, intracluster hot gas, magnetic fields and relativistic particles) and the effect of the environment on their evolution. On larger scales, samples of clusters are very useful tools to understand the formation and evolution of large-scale structure through the study of the average statistical properties of clusters as a function of redshift. Since clusters are relatively luminous at many wavelengths, they may be more easily traced to very high redshift (even though there are not many clusters known beyond $z \geq 1$) and thus they represent a very important observational tool for cosmologists. In particular, they can be used to constrain cosmological parameters.

All this explains the past and present efforts made in cluster surveys to build very large cluster samples and to push the detection of clusters to higher and higher redshift. In this respect the search for clusters has greatly benefitted from new technologies and observational capabilities. Faint spectroscopic data from Keck and VLT, deep optical and near-infrared imaging in space (HST) and from the ground, observations of the intracluster medium with ROSAT and ASCA, enhanced imaging and spectroscopic capabilities of Chandra and XMM-Newton, have considerably added to our knowledge of these objects.

Cluster searches are conducted in different waveband domains. The traditional searching waveband for clusters has been the optical wavelength, but in the last twenty years X-ray searches have played an increasingly important role. More recently radio, infrared and submm searches have also been successfully used to detect bright clusters. All cluster finding methods, in any waveband domain, suffer from selection effects and biases. What is important is to be aware of the selection effects and to be able to correct for the biases. It is also desirable to have catalogs extracted from as many different wavelength domains as possible, since each sample will contain a somewhat different cluster population with different selection effects. Here is an (incomplete) list of all-sky or extra-galactic surveys carried out at different wavelengths. Most of these surveys appeared in the literature in the past decade. Cluster studies have greatly benefitted from these surveys even if several of them were not specifically designed to search for such systems.

POSS and SERC (and related digitized surveys)

ROSAT ¹¹⁹

NVSS ²¹

FIRST ³

WENSS ⁹³

IRAS ¹⁰⁰

IRAS PSCz Redshift Survey ¹⁰¹

CFA redshift survey ^{58, 29, 59}

2dFGRS ¹⁹

6dF ²⁰

LCRS ¹⁰⁸

NBG groups of galaxies ¹¹³

VIRMOS ⁶⁹

ESP ¹¹⁸

SUMSS ⁵

2MASS ⁶⁰

DENIS ⁷⁷

SDSS ^{64, 78}

Readers are referred elsewhere for details on each survey. Here I will mention only the Sloan Digital Sky Survey (SDSS), which is an ambitious project involving a joint venture of several astronomical institutes.

1.1 The Sloan Digital Sky Survey (SDSS)

The Sloan Digital Sky Survey⁶⁴ will eventually produce a map of 10,000 \square° of the northern sky and 225 \square° of the southern sky. The SDSS is both a photometric (five-bands: u' , g' , r' , i' , z') and a spectroscopic survey which will permit the selection of galaxy clusters using well-defined, automated algorithms. Cluster investigations will greatly benefit from the SDSS data, either alone or in combination with other wavelength datasets, from measurements of cluster parameters to correlations between cluster properties and their evolution. The very large volume and objective identification methods of the SDSS will result in a uniform database of objects including an enormous sample of clusters. This sample can be used to characterize the cluster population statistically with great accuracy. It will also allow to test the cosmological models through the measure of galaxy clustering and to characterize the large-scale structure at the present epoch ($z < 0.2$).

2 Cluster Surveys and Catalogs in Optical

In the years following the pioneering work of Abell¹, only a few surveys were produced to search systematically for clusters of galaxies. The early generation systematic surveys^{1, 2, 123} were done by visual inspection of plates and thus with no quantifiable selection functions. The Abell catalog was for many years the only cluster catalog available and thus heavily used for cluster studies, including discovery of superclusters, and large-scale structure investigations up to $z \leq 0.2$. At higher redshift ($z < 0.5$) surveys based on prime focus deep plates^{50, 22} have provided information on galaxy evolution, on galaxy clustering and space densities as a function of richness, on the Butcher-Oemler effect, etc. But the real breakthrough was the emergence of optical cluster catalogs with completely automated selection and quantifiable selection criteria (see among others^{107, 73, 26}). The automated surveys increased the efficiency of cluster searches and allowed more accurate determinations of cluster space density measurements. At even higher redshifts ($z \geq 0.5$) it becomes extremely difficult to detect enhancements in the galaxy surface density against the overwhelming field galaxy population and optical surveys are known to suffer from effects of superpositions of unvirialized systems (see among others⁴¹ and¹¹⁴). Essentially all optical surveys still use richness, either in two dimensions or three dimensions, as the selection criterion, but richness correlates poorly with mass because of the projection effects. Fully automated and objectively selected catalogs of clusters with quantifiable selection criteria (different from the traditional $\delta\rho/\rho$) are thus necessary for these catalogs to be statistically useful.

I will discuss now current efforts that should have a significant impact on optical/NIR cluster studies.

2.1 The Palomar Distant Cluster Survey (PDCS)

The number of known distant clusters has greatly increased since the publication in 1996 of the PDCS catalog by Postman and collaborators⁹¹. The PDCS is among the first fully automated objectively selected catalog of clusters based on CCD imaging data. The investigators use a matched filter algorithm, in both positional and photometric data, to search for overdensities in the galaxy distribution. The 79 clusters and candidates in the original survey paper⁹¹, of which 16 were already known from the catalog of Gunn, Hoessel and Oemler⁵⁰, cover the redshift range $0.2 < z < 1.2$. One of the main results of the survey is that the PDCS cluster space density is a factor of about five above that seen in the local universe as measured from the Abell catalog. Recently this result was confirmed by a spectroscopic survey of the PDCS clusters in the redshift range $0.1 < z < 0.35$ ⁵⁷. Actually it was found that a fraction ($\sim 1/3$) of the PDCS clusters have lower velocity dispersions (200 km s^{-1} , typical of groups) but richness appropriate for clusters. Excluding those low velocity dispersion clusters the PDCS cluster density estimate is of ~ 3 times that of the Abell catalog for equivalent mass clusters of galaxies, in agreement with the APM^{76, 27} and the Edinburgh-Durham cluster catalog¹⁰, thus raising the possibility that the Abell catalog is incomplete. These results are different from the results of the X-ray surveys which find incompleteness at a given luminosity to be only 30%^{36, 37, 30}.

Oke and collaborators⁸⁴ performed extensive spectroscopic observations with Keck to get spectra for 9 distant PDCS clusters ($z > 0.6$). They measured over ~ 100 redshifts per cluster for galaxies with $R \leq 23.3$. A contamination of 30% was found in the spectroscopic survey which led the authors to conclude that optical detection of clusters remains a successful and important method for identifying such systems out to $z \sim 1$ (even if it suffers from projection effects) and that it will provide an important complement to cluster searches at other wavelengths. Recent findings from the Keck spectroscopic survey of the 9 PDCS clusters include the discovery of a group-group merger at $z=0.84$ ⁷¹ and the optical detection of a supercluster at $z \sim 0.91$ ⁷².

2.2 The ESO Imaging Survey (EIS) Clusters

The matched-filter algorithm of Postman and collaborators was applied to the EIS^{94,24} database, in its original version (see^{85, 86, 104}) and in a modified version (see⁷⁰). The EIS is a public imaging survey, carried out by ESO and its community, to provide target lists for the Very Large Telescope. Among the goals of the EIS was the construction of a catalog of distant cluster candidates over a wide range in redshift from which targets could be drawn for subsequent follow-up studies. Different groups^{70, 92, 87} are involved in the spectroscopic follow-up to confirm the cluster nature through spectroscopy. Preliminary results¹⁰⁴ show overdensities of red objects detected in over 300 group and cluster candidates in $17 \square^\circ$. The estimated redshifts are in the range $0.2 < z < 1.3$ with a median redshift of $z \sim 0.5$. This is the largest sample of medium-distant clusters available in the southern hemisphere.

2.3 The Low-Surface-Brightness Fluctuations in the Background Sky

An interesting approach to find distant clusters is the one adopted by Dalcanton²⁵ and by Zaritsky and collaborators¹²². These investigators use an old idea by Shectman^{105, 106}, that the optical background light can be used to obtain information about the underlying distribution of galaxies. They detect the light from the unresolved galaxies in a cluster which manifest themselves as low-surface-brightness fluctuations. Extremely accurate flattening of the sky is required, but can be achieved with telescopes operating in drift-scan mode (like the great circle camera on the Las Campanas 1m telescope). The advantage of this technique is that many square degrees of sky can be surveyed in only a few nights using relatively small telescopes since dramatically shorter exposure time than for traditional surveys is required. Of course deeper follow-up imaging is necessary for confirmation of the candidates plus spectroscopy for redshift determination. An initial set of 10 cluster candidates, out of a preliminary list of 52 objects from a drift-scan survey (the Palomar Transit Grism Survey²⁵) of only $17.5 \square^\circ$ of the northern sky, were confirmed as bona-fide clusters through imaging and spectroscopy. The cluster redshifts range from 0.4 to 1.06. From a larger southern survey ($\sim 130 \square^\circ$ of the sky performed at Las Campanas Observatory) a catalog of over 1000 candidate clusters and groups has been produced. The latest results of the LCO survey are described by Dennis Zaritsky in these proceedings.

2.4 Toronto Red-Sequence Cluster Survey (RCS)

The Red-Sequence Cluster Survey (RCS)⁴⁹ is motivated by the observation that all rich clusters have a population of early type galaxies which follow a strict color-magnitude relation. While the properties of the overall cluster galaxy population do evolve with redshift (i.e. the blue fraction is generally higher at higher redshift), in all well-formed clusters so far observed there is a red sequence population not generally found in the field when looking over a large redshift range. Thus the searching algorithm is constructed to exploit the red sequence of early-type galaxies as a direct cluster indicator. The method has been tested using both real redshift survey data and thorough simulations. The RCS is designed to provide a large sample of optically selected clusters between $0.1 < z < 1.4$ by imaging $100 \square^\circ$ in two filters (R and z') to a depth sufficient to find galaxy clusters at $z \sim 1.4$. The RCS survey observations started in May of 1999, but initial analysis of about $6 \square^\circ$ of data has already allowed the discovery of numerous cluster candidates that can be viewed at <http://www.astro.utoronto.ca/~gladders/RCS/>.

2.5 The Canadian Network for Observational Cosmology (CNOC)

A particular mention goes to the CNOC projects. The CNOC survey^{120, 13} consists of spectrophotometric observations of 15 intermediate redshift and high luminosity EMSS clusters ($0.1 < z < 0.6$; $L_X > 4 \times 10^{44} \text{ erg s}^{-1}$) and, as such, it is not an effort aimed at finding new

clusters of galaxies. The overall goal was to measure the total mass and luminosity in the central virialized region of the clusters to establish the value of Ω and measure any biases among cluster galaxies, cluster mass, and field galaxies. The survey developed into two separate projects: the CNOC1, which is a galaxy cluster redshift survey containing over 2600 velocities used to measure Omega through the cluster dynamics; and the CNOC2¹²¹ which is a field galaxy redshift survey containing about 6000 velocities to measure the evolution of galaxy clustering and galaxy populations. Both surveys are used by the scientific community at large for cosmological studies.

2.6 Radio and Near-Infrared Selection

It was realized several years ago that luminous radio galaxies at redshift $z \sim 0.5$ inhabit rich clusters⁵⁶. There is now growing evidence that at higher redshifts ($z \geq 3$) powerful radio sources are located at the center of forming clusters⁹⁰. Observational indications manifest as detection of luminous extended X-ray emission around the radio galaxies^{31, 23}, overdensities selected by infrared color³², searches around powerful Ultra-Steep Spectrum high-redshift radio galaxies^{14, 15, 89}, spectroscopic studies³², detection of companion galaxies with narrow-band imaging⁷⁹, large Faraday depolarization and rotation measures of the radio sources⁴ and so on. Two examples are: MRC 0316-257 at $z=3.12$ ⁶⁸, 1138-262 at $z=2.2$ ^{89, 65}. Other searches have shown overdensities of distant objects in fields around weak steep spectrum radio galaxies (e.g. 53W002 at $z=2.390$ ^{88, 63}). From these observational results it is clear that searches around high redshift radio galaxies are a good alternative to optical searches for finding very distant clusters of galaxies. Another interesting alternative to locate high redshift structures are searches in fields of multiple lens quasars, as demonstrated by the triple quasar MG2012+112 at $z=3.26$, where a distant cluster at $z \sim 1$ has recently been discovered¹⁰⁹. However, it must be noted that these techniques do not provide statistically complete samples of distant clusters.

In more recent years the near infrared has emerged as a new efficient band to find distant clusters. Stanford *et al.* (1997)¹¹⁰ have shown that optical-IR colors (very red J-K colors) can be used to enhance the contrast of the cluster galaxies against the field galaxy population and, at the same time, to estimate the cluster redshift (e.g. CIG J0848+4453 at $z=1.273$)¹¹⁰.

To summarize this first part of the review:

Our knowledge of cluster properties (such as richness, morphology, space density, velocity dispersion, optical luminosity, morphological content etc.) and all correlations between these properties and their evolution (like Butcher-Oemler effect, space density as a function of redshift, optical morphology, etc.) has greatly improved in the last decade. The use of well-defined, automated algorithms has allowed us to catalog a continuous range of galaxy overdensities from rich clusters down to poor groups. Near-infrared and radio selections have pushed the detection of such systems to higher redshifts. The nearby surveys with their derived catalogs have contributed significantly to our understanding of the local universe and of the large-scale structure and have allowed comparisons with galaxy clusters up to large look-back times ($z \geq 1$). The modern 8m-10m telescopes are, and will be, used to study the formation and evolution of the most distant galaxies and clusters. By studying these objects, their mass, distribution and evolution we will obtain vital information on the formation history of the underlying mass field which is a fundamental goal in cosmology.

3 Cluster Surveys and Catalogs in X-rays

I have been advocating for many years the X-ray selection as an efficient method to find clusters of galaxies. The detection of X-ray emission is one of the cleanest ways to avoid sample

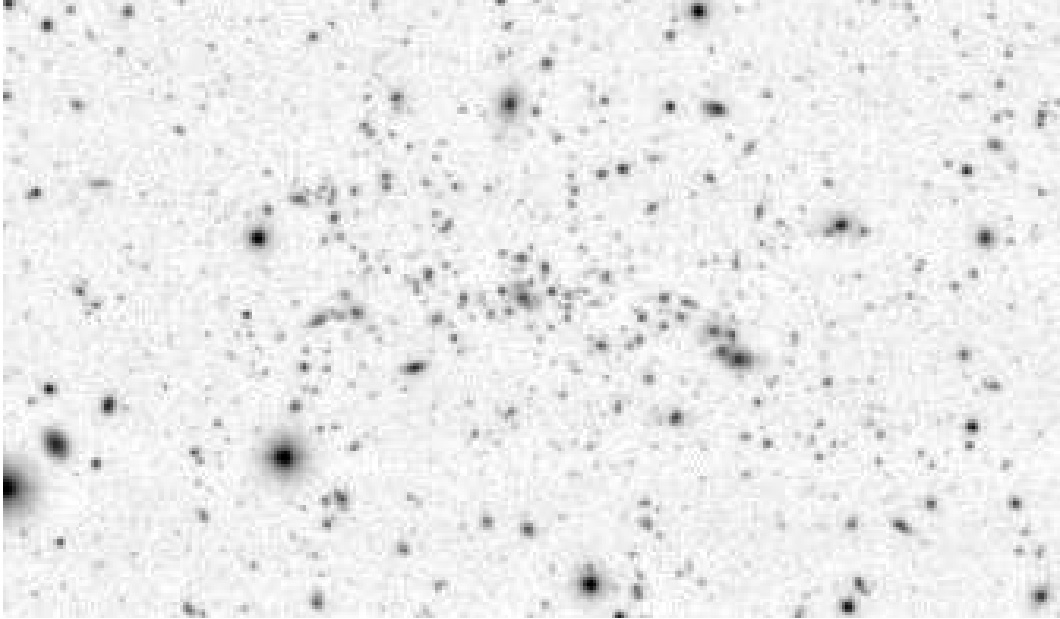


Figure 1: Subarray I image of MS 1054–03 at $z = 0.83$ taken with the Tek 2048 CCD camera at the University of Hawai'i 2.2m

contaminations, especially in the selection of high- z clusters. For the last several years X-ray cluster detection has been considered superior to classical optical detection methods because:

- Clusters are powerful X-ray emitters with temperature and gas density which reflect the cluster gravitational potential
- L_X scales as the square of gas density so projection effects are minimized
- Confusion from background fluctuations is much less prevalent than in the optical
- While in the optical the definition of cluster shape and mass with galaxy number counts and redshifts is limited by the number of cluster galaxies, in X-rays the measurements are only limited by the number of photons received
- Selection criteria are objective and quantifiable.

Naturally to unambiguously identify genuine distant clusters ($z > 0.5$), besides the evidence for hot gas through detection of X-ray emission, other criteria should hopefully be fulfilled like: measurement of projected overdensity of galaxies combined with significant overdensity observed in the redshift distribution, evidence for peak mass distribution, either from weak or strong lensing and so on. Several new cluster lens systems have been discovered in X-ray selected samples^{67, 74} and several weak lensing studies are using X-ray selected clusters (see⁸⁰ for a review).

The first X-ray imaging instruments onboard the Einstein Observatory allowed the construction of the EMSS (Extended Medium Sensitivity Survey) catalog of clusters^{42, 111, 53}. EMSS clusters are still observationally followed-up today. The cluster *MS 1054 – 03*⁴⁴ is certainly one of the most amazing clusters known. At a redshift of 0.83⁴⁴, with a temperature of 12.4 keV³³ and a mass of $7 \times 10^{14} h^{-1} M_{\odot}$ ³³, the existence of massive clusters at $z \sim 1$ is no longer in doubt (see Fig. 1). All the X-ray surveys of the last decade, except for the EMSS, have been carried out using ROSAT¹¹² data, either from the All-Sky Survey (RASS¹¹⁹) or from pointed observations. The surveys belonging to the former group, the contiguous area surveys, cover a very large solid angle ($\sim 10,000 \text{ } \square^{\circ}$ or more, with the exception of the NEP⁴⁷) but are shallower than the pointed data surveys. The contiguous area surveys can be used to examine

large-scale structure in the cluster distribution but they cannot detect in great number the most massive and luminous systems at high redshift ($z > 0.3$), with perhaps the exception of MACS 38 (see next section). The great advantage of the serendipitous surveys, those extracted from the pointed data, is their much deeper sensitivity, about two orders of magnitude deeper than the contiguous area surveys ($\sim 1 \times 10^{-14}$ vs $\sim 1 \times 10^{-12}$ erg cm $^{-2}$ s $^{-1}$ in the ROSAT band), even though their solid angle is less than ~ 200 \square° , which makes them insensitive to massive clusters in great number.

The REFLEX^{6, 51}, NORAS⁷, BCS³⁶ (and its extension eBCS³⁷), RASS1-BS³⁰, MACS³⁸ and NEP^{9, 81, 47} belong to the group of contiguous area surveys. While the RDCS^{96, 97}, Southern SHARC^{11, 18} and Bright SHARC⁹⁵, WARPS^{102, 61, 39}, CFA 160 \square° ^{115, 117} and BMW^{66, 12} are serendipitous cluster surveys.

4 The Contiguous Area Surveys

The contiguous area surveys, and in particular the all sky surveys, are good tracers of large-scale structure given the large solid angle sampled and the sizes of the superstructures (several hundreds of Mpc). The selection through X-ray emission has the additional advantage of a more direct relation between luminosity and mass and thus the derived X-ray luminosity function is most closely related to the mass function of the clusters which is used as an important calibrator of the amplitude of the density fluctuation power spectrum. The surveys described below, except for MACS, sample the nearby universe ($z < 0.3$) and are used as excellent reference for cluster studies at higher redshift. Deeper surveys, like the NEP, are not restricted to the local universe. The NEP has allowed the discovery of distant clusters, like *RX J1716 + 66*^{46, 55} at $z = 0.81$, a filamentary system very similar in many aspects to the better known cluster *MS 1054 – 03* (see Fig. 2).

4.1 The REFLEX and NORAS Galaxy Cluster Surveys

There are two X-ray cluster surveys covering both celestial hemispheres: the Northern Rosat All-Sky (NORAS⁷) survey and the complementary survey in the southern hemisphere, the REFLEX (Rosat Eso Flux Limited X-ray survey^{6, 51}). Both projects are carrying out the optical follow-up and redshift determination of clusters selected from the ROSAT All-Sky survey. While the NORAS cluster sample selection is purely based on X-ray information (e.g. extent of the X-ray source), the REFLEX survey is based on the correlation of X-ray sources with galaxy overdensities. Recent results from the REFLEX include a measure of the power spectrum within a cubic volume of $400h^{-1}$ Mpc side and an estimate of the two-point correlation function⁵². Hans Böhringer (these proceedings) will describe each survey in detail.

4.2 The ROSAT Brightest Cluster sample (BCS), the RASS1 Bright Sample (RASS1-BS) and the Massive Cluster Survey (MACS)

The BCS, RASS1-BS and MACS cluster samples are all compiled from the ROSAT All-Sky Survey data.

The BCS³⁶ is an X-ray flux limited sample which comprises 203 clusters in the northern hemisphere ($\delta \geq 0$ and $|b| \geq 20^\circ$) with measured redshifts $z \leq 0.3$. The sample is complete down to 4.4×10^{-12} erg cm $^{-2}$ s $^{-1}$ in 0.1–2.4 keV. The clusters have been selected from the RASS data using the Voronoi Tessellation and Percolation algorithm (VTP³⁵) optimized for the detection of irregular and extended X-ray sources. The BCS extension, the eBCS³⁷, comprises 107 X-ray selected clusters with fluxes $\geq 2.8 \times 10^{-12}$ erg cm $^{-2}$ s $^{-1}$ (0.1–2.4 keV) and measured redshifts $z \leq 0.3$. Combining the two samples (310 clusters) there are signs of large-scale structure in the z -histogram at $z \sim 0.036$ and $z \sim 0.077$ ³⁷.

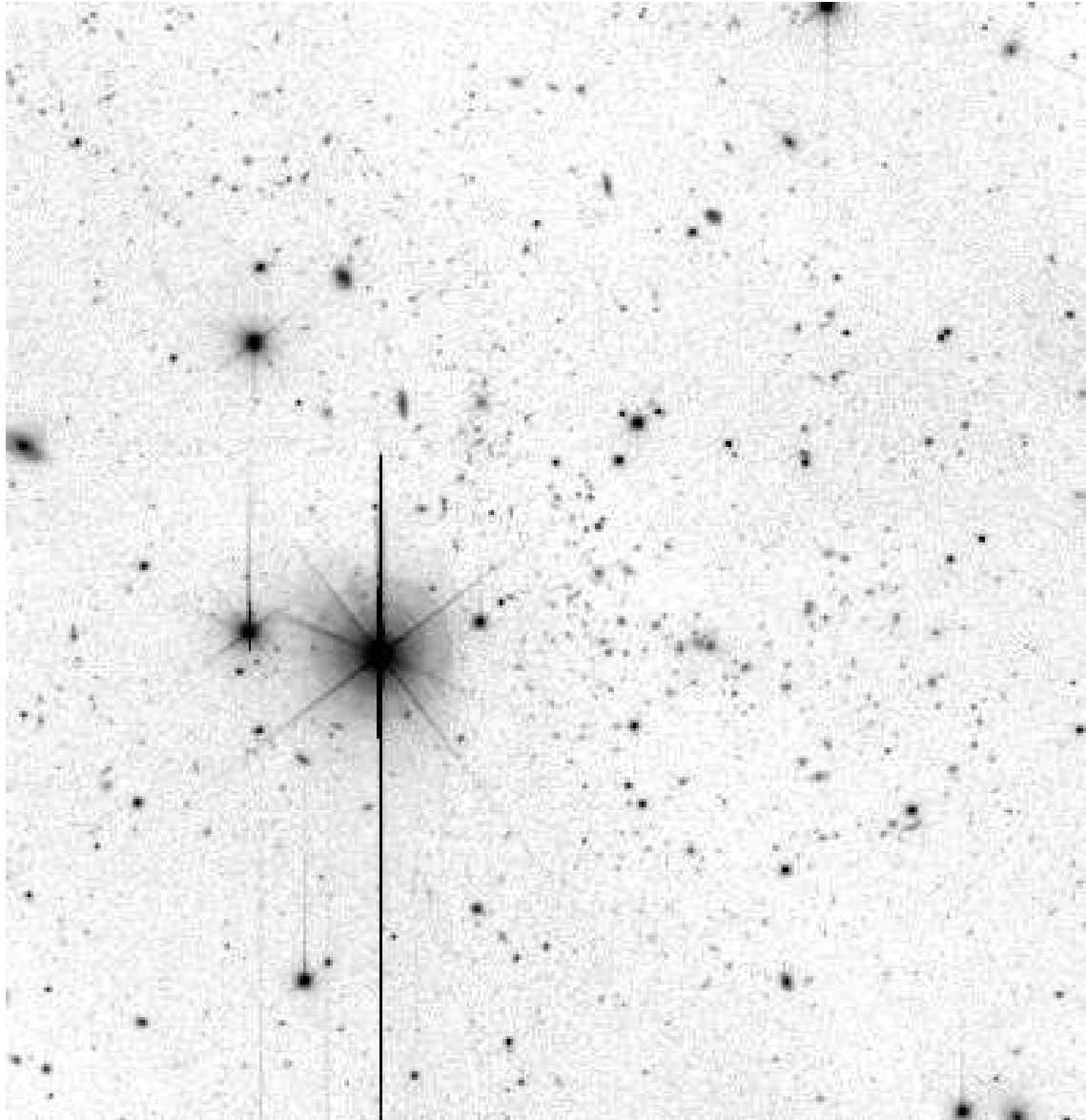


Figure 2: Subarray I image of the NEP cluster *RXJ1716+66* at $z = 0.81$ taken with the University of Hawai'i $\times 8K$ CCD mosaic camera on the CFHT prime focus

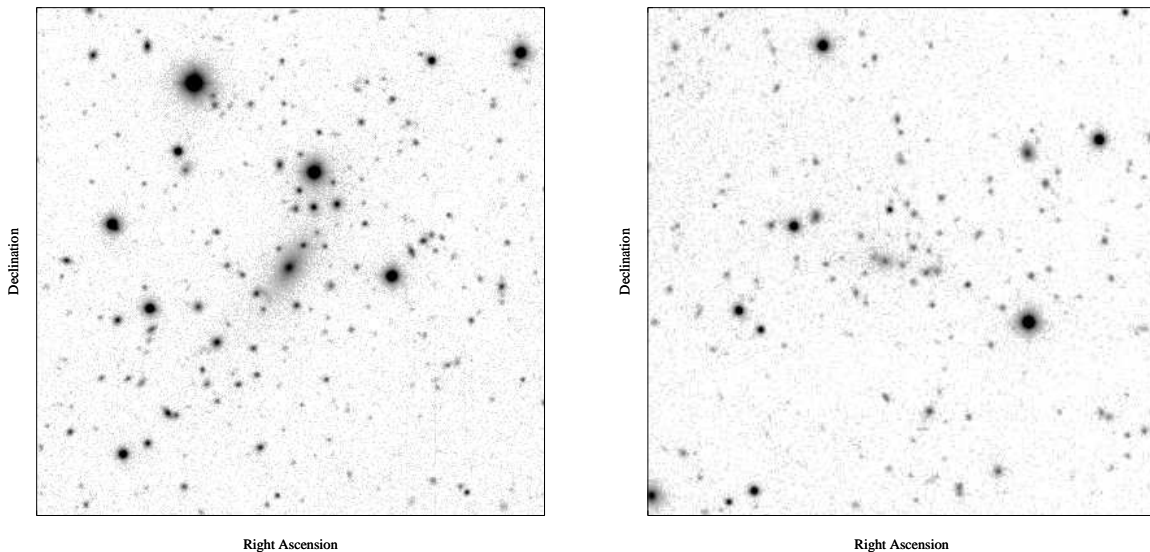


Figure 3: R band images of MACS clusters obtained with the University of Hawaii’s 2.2m telescope. Left: one of the most nearby and least X-ray luminous clusters in the MACS sample ($z = 0.329$, $L_X = 6.4 \times 10^{44}$ erg s $^{-1}$, 0.1–2.4 keV). Right: One of the most distant and more X-ray luminous clusters in the MACS sample ($z = 0.570$, $L_X = 1.7 \times 10^{45}$ erg s $^{-1}$, 0.1–2.4 keV). Both clusters are new discoveries. The shown images span $1 h_{50}^{-1}$ Mpc on the side at the cluster redshift.

The other survey of bright clusters from the RASS is the RASS1 Bright Sample³⁰ in the southern hemisphere. The RASS1-BS is a flux limited sample of clusters that uses the Steepness-Ratio Technique, SRT³⁰, which takes into account the extended nature of the X-ray emission of sources. The final sample is count-rate limited and thus the completeness in flux varies between ~ 3 and 4×10^{-12} erg cm $^{-2}$ s $^{-1}$ in the hard 0.5 – 2 keV band. It covers a total area of 8324 \square° and includes 130 clusters of which 126 with measured z (< 0.3). Both the BCS and the RASS1-BS have allowed an accurate determination of the bright end of the logN–logS and of the local cluster X-ray luminosity function over almost three decades in X-ray luminosity. Both RASS samples provide an important reference for searches for cluster evolution at higher redshift. There are of course many clusters in common between the last two surveys and the previous section surveys since all of them are based on X-ray detections in the RASS.

The third cluster survey compiled from RASS data, the MACS³⁸, is still work in progress. The main characteristic of the survey is a very large solid angle ($\sim 23,000 \square^\circ$) combined with a flux limit of 1×10^{-12} erg cm $^{-2}$ s $^{-1}$ in 0.1–2.4 keV. Clusters are selected from the RASS Bright Source Catalog (BSC¹¹⁹) on the basis of the X-ray hardness ratio and with $|b| \geq 20^\circ$ and $-40^\circ \leq \delta \leq 80^\circ$. The survey has provided so far the largest sample of clusters of galaxies at all redshifts (more than 850 clusters of which 755 with spectroscopic redshifts³⁸). About 88 of such systems are in the range $0.3 \leq z \leq 0.6$ (see Fig. 3 for two MACS clusters at $z = 0.329$ and $z = 0.57$). Preliminary results from the MACS, based on a subsample of 25 X-ray brightest clusters, show that negative evolution of the X-ray luminosity function is not significant at luminosities $L_X > 1 \times 10^{45}$ erg s $^{-1}$ out to redshifts of $z \sim 0.4$ ⁴⁰ (see section 6 for a discussion on cluster evolution).

4.3 The North Ecliptic Pole survey (NEP)

The last survey based on the ROSAT All–Sky survey data is the NEP^{54, 45, 81, 47}, a unique survey in its X-ray depth and contiguous sky coverage. The NEP uses data from the deepest region of the RASS, where the scan circles converge and the effective exposure time approaches

40ks, to produce a complete and unbiased X-ray selected sample of distant clusters. The survey covers $81 \square^\circ$ down to a flux limit of $\sim 3 \times 10^{-14} \text{ erg cm}^{-2} \text{ s}^{-1}$ in the 0.5–2.0 keV band. There are 445 sources detected at $> 4\sigma$ in the 0.1–2.4 keV band. Sixty-four of these sources are identified with clusters, 19 of which have a redshift greater than 0.3 with the highest at $z=0.81$. The goal of the survey was a better understanding of the nature of cluster evolution and a characterization of the three dimensional large-scale structure of the universe by studying the cluster-cluster correlation function. A supercluster of 21 groups and clusters has indeed been found during the analysis of the NEP sources⁸². Unlike most of the cluster surveys that are based on X-ray cluster detections the NEP strategy is to identify through spectroscopic observations *all* the detected sources independently from their extension and nature. Comparing the number of the observed clusters in the NEP survey with the number of expected clusters assuming no–evolution models there is a deficit⁴⁷ of clusters with respect to the local universe which is significant at $> 4.7\sigma$. The evolution appears to commence at $L_{0.5-2} > 1.8 \times 10^{44} \text{ erg s}^{-1}$ in the NEP data. This result is in agreement with the original EMSS results^{43, 53} (see next section).

5 The Serendipitous Cluster Surveys

In the context of cluster evolution the X-ray luminosity function (XLF) is a relevant quantity which parameterizes the number density of clusters per unit volume per luminosity interval. The main result of the EMSS⁴² cluster sample was the evidence for cluster XLF evolution at the 3σ level. This evolution, dubbed negative evolution, goes in the sense that there are fewer^{43, 53} distant clusters but only at luminosities $L_{0.3-3.5} > 5 \times 10^{44} \text{ erg s}^{-1}$. This behavior is expected in hierarchical formation theories where the most massive clusters form last. This early result inspired many EMSS–style cluster surveys, all based on ROSAT archival deep pointings. The issue of “evolution versus no-evolution” became a controversial and very hotly debated issue in the X-ray cluster community. Each one of the EMSS–style cluster surveys described below covers an area of sky of less than $200 \square^\circ$, much less than the $\sim 800 \square^\circ$ of the original EMSS, but with sensitivities almost an order of magnitude deeper than the EMSS ($\sim 1.8 \times 10^{-14} \text{ erg cm}^{-2} \text{ s}^{-1}$ vs $\sim 1.3 \times 10^{-13} \text{ erg cm}^{-2} \text{ s}^{-1}$ in 0.3–3.5 keV). Most of these surveys are still works in progress but a few preliminary results are available. While everybody agrees on the XLF of clusters with $z < 0.3$ and $L_{(0.5-2)} < 3 \times 10^{44} \text{ erg s}^{-1}$, there is not a consensus yet for the XLF of the brightest and most distant clusters known. As with the contiguous area surveys, several clusters are common to the surveys described below since all the surveys use the same pointed ROSAT data.

5.1 The Rosat Deep Cluster Survey (RDCS)

The RDCS^{96, 97} was designed to compile a large, X-ray flux-limited sample of galaxy clusters, selected via a serendipitous search for extended X-ray sources in ROSAT-PSPC deep pointed observations. The depth and the solid angle of the survey were chosen to probe an adequate range of X-ray luminosities over a large redshift baseline. Approximately 160 candidates were selected down to the flux limit of $1 \times 10^{-14} \text{ erg cm}^{-2} \text{ s}^{-1}$ in 0.5–2.0 keV, over a total area of $50 \square^\circ$, using a wavelet detection algorithm. This technique is particularly efficient in discriminating between pointlike and extended, low-surface-brightness sources⁹⁶. The RDCS has not been completely identified yet but complete subsamples have been created to allow a statistical reconnaissance of the data. The most interesting finding, beside the detection of an X-ray selected cluster at $z=1.26$ (*RX J0848.9 + 4452*⁹⁸), is the confirmation of the EMSS results: the most luminous, presumably most massive clusters are indeed rarer at high redshift^{99, 8}.

5.2 *The Wide Angle Pointed Rosat Survey (WARPS)*

The goal of the WARPS, as with all the other serendipitous surveys, was to compile a complete, unbiased, X-ray selected sample of clusters of galaxies from serendipitous detections in deep, high-latitude ROSAT PSPC pointings^{102, 61}. The detection algorithm employed is the VTP algorithm, particularly suited for detection of low-surface-brightness emission sources. Optical follow-up is not restricted to the obvious extended sources but includes also point-like sources in order to be as complete as possible in the detection of possible unresolved clusters. The survey is still work in progress and as of today the WARPS covers $73 \square^\circ$ down to a flux limit of 5.5×10^{-14} erg cm⁻² s⁻¹ in 0.5–2.0 keV³⁹. There are about 150 clusters, half of which at $z > 0.3$, in the luminosity range from 10^{42} to 8×10^{44} erg s⁻¹. A comparison of the WARPS XLF with the local BCS luminosity function does not show any evidence for luminosity evolution up to $z=0.83$ ⁶².

5.3 *The Serendipitous High-Redshift Archival Rosat Cluster surveys (Southern SHARC and Bright SHARC)*

The southern SHARC survey consists of 35 clusters of galaxies discovered as extended sources at a flux limit of $\simeq 3.9 \times 10^{-14}$ erg cm⁻² s⁻¹ in 0.5–2 keV in less than $20 \square^\circ$ of sky¹⁸. There are 16 clusters in the redshift range $0.3 < z < 0.7$ detected in 66 deep ROSAT PSPC pointings¹¹. No evidence for evolution^{18, 11} of the XLF over the luminosity range $L_X \sim (0.3 - 3) \times 10^{44}$ erg s⁻¹ in 0.5–2.0 keV is found, in agreement with the XLF of the low redshift cluster population. However, the SHARC sample is not able to test the high luminosity-high redshift space where the XLF evolution was detected.

The Bright SHARC survey⁹⁵ is the largest of the serendipitous surveys covering $178 \square^\circ$ of sky. The survey uses a wavelet based algorithm and detects 374 extended sources in deep ($t_{exp} > 10$ ks) PSPC pointings. The brightest 94 sources above a flux limit of 1.4×10^{-13} erg cm⁻² s⁻¹ in 0.5–2 keV constitute the Bright SHARC cluster candidate sample. Optical follow-up has identified 37 clusters of which 12 in the range $0.3 < z < 0.83$. Adding to the SHARC sample the $160 \square^\circ$ sample (see below) the authors⁸³ present evidence for a deficit of clusters at $L_X > 5 \times 10^{44}$ erg s⁻¹ compared to what is expected from a non-evolving XLF.

5.4 *The CFA 160 \square° survey*

The $160 \square^\circ$ X-ray catalog¹¹⁵ was constructed by detecting significantly extended X-ray sources in 653 ROSAT PSPC pointed observations. After the Bright SHARC it is among the largest of the new serendipitous surveys and comprises 203 clusters (with redshift measurements for 100 X-ray brightest clusters¹¹⁷). The X-ray detection is performed in a fully automated and objective way and selection effects are well understood. Given the large area combined with high sensitivity the $160 \square^\circ$ survey is particularly suited to probe the evolution of the bright end of the cluster XLF ($L_X > 3 \times 10^{44}$ erg s⁻¹ in 0.5 – 2 keV band). A calculation of the XLF in the redshift interval $0.3 < z < 0.8$ (37 clusters with $f_X > 1.4 \times 10^{-14}$ and $L_X > 0.71 \times 10^{44}$ erg s⁻¹) shows a deficit¹¹⁷ of high luminosity clusters in agreement with the EMSS XLF^{43, 53}.

5.5 *The Brera Multiscale Wavelet survey (BMW)*

The BMW^{66, 12} is the most recently initiated survey and it is still work in progress. The BMW is the only serendipitous survey which applies a wavelet detection algorithm, first used by the RDCS, to analyze images taken with the ROSAT HRI instrument rather than the PSPC. Analysis of a large set of HRI data will allow the investigators to survey $\sim 400 \square^\circ$ down to a limiting flux of $\sim 1 \times 10^{-13}$ erg s⁻¹ cm⁻², and a much smaller volume ($\sim 0.3 \square^\circ$) down to $\sim 3 \times 10^{-15}$ erg cm⁻² s⁻¹. A complete catalog will result from their analysis, consisting of the BMW Bright Source Catalog (BMW-BSC), with sources detected with a significance of

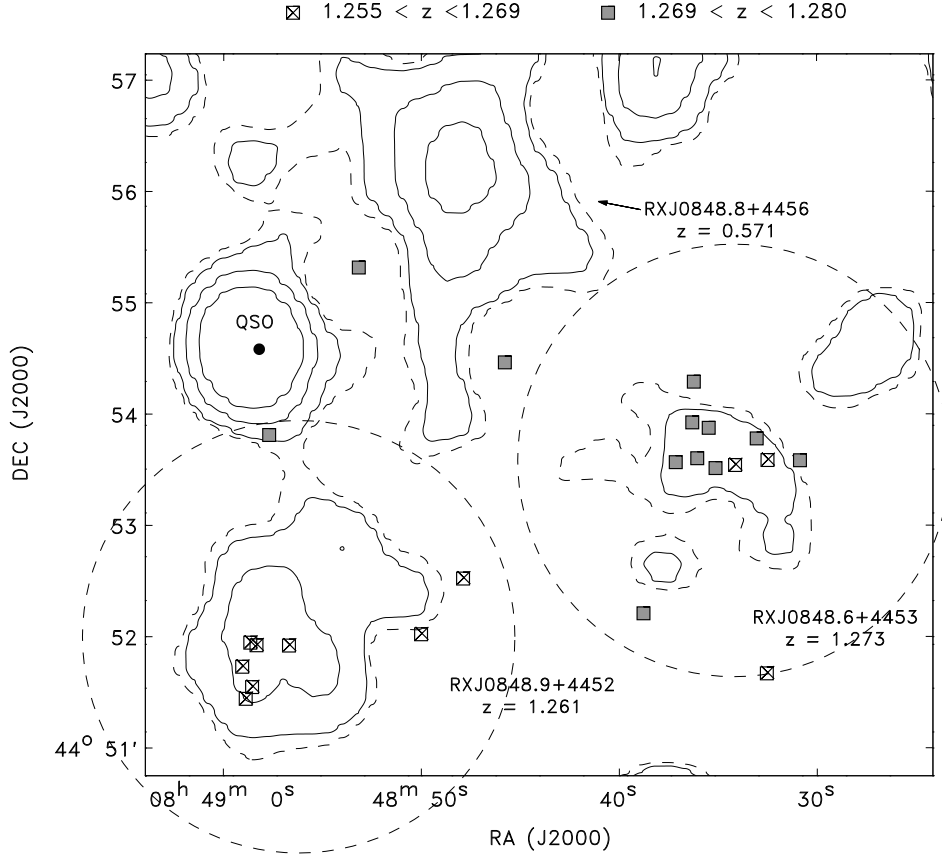


Figure 4: Adapted from Fig. 6 in Rosati *et al.* 1999; original caption reads: Lynx field overlaid ROSAT-PSPC contours and spectroscopic members. The circles are centered at the X-ray centroids of the two clusters with a radius of $116' = 1h_{50}^{-1} Mpc$ at $z = 1.27$. Filled squares refer to clusters with $1.255 < z < 1.269$, and squares with crosses refer to clusters with $1.269 < z < 1.280$.

$\geq 4.5\sigma$ and the Faint Source Catalog (BMW-FSC), with sources at $\geq 3.5\sigma$. At present there are about 300 cluster candidates (Guzzo, private communication) which are being imaged at optical telescopes for confirmation. The survey is at a too early stage to give any indication of the behavior of the high-luminosity, high-redshift galaxy clusters.

6 Final Remarks

Many statistical and individual cluster studies have been made in the last decade. This has been possible thanks to the operation of larger and more sensitive telescopes either ground based and in space. In X-rays more accurate observable and derived cluster properties (like flux, luminosity, gas density profiles, gas temperatures, cluster gas and total mass, etc.) and their relations (like the luminosity-temperature or the mass-temperature relations) are now available. Mass determinations from studies of velocity dispersion and from weak lensing are in good agreement with mass derivations from X-ray temperatures measurements. We have a better understanding of the effect of the environment on cluster properties (i.e. presence of cooling

flows, extended radio lobes, clumpiness seen in optical and IR, morphological content of galaxies, etc.).

The sensitivity of the X-ray surveys is comparable to other wavelength sensitivities and clusters can be detected out to $z > 1$ ⁹⁸. Detailed studies of high- z massive clusters have shown that they are filamentary in optical with the X-ray emission following the elongation of the optical galaxies^{33, 46, 39}. Most high- z clusters have high velocity dispersions (when many redshift measurements are available) as well as high gas temperatures^{33, 48}. Three out of four X-ray selected clusters at $z \sim 0.8$ are not relaxed (*RX J1716+66*^{46, 16, 55} at $z = 0.81$; *MS 1054-03*^{33, 75} at $z = 0.83$; *RX J0152-13*^{28, 39} at $z = 0.83$ and *MS 1137+66*^{34, 17} at $z = 0.78$, this last one is well compact and unrelaxed). The rarity of relaxed systems in high- z clusters may indicate that we are beginning to observe the formation epoch of the majority of massive clusters.

Progress has been made in the detection of large-scale structure both nearby⁸² and out to $z \sim 1.27$ (see Fig. 4 here and the beautiful color image of the Lynx field in Rosati et al. 1999⁹⁸, their Fig. 7). Also a possible detection of X-ray emission from an intra-cluster filament has been reported¹⁰³.

There is accumulating evidence in favor of negative evolution, that is less high- z high luminous clusters in the past. All the new serendipitous surveys, except for the WARPS, are now reporting mild negative evolution at varying levels of significance. However, given the small number statistics and incomplete optical follow-ups of some existing serendipitous clusters surveys, the issue has not been completely resolved yet. The high throughput and energy resolution of the large X-ray telescopes now in orbit, Chandra and XMM-Newton, will allow to obtain more reliable flux measurements which will help reduce some of the systematic uncertainties in the derived XLF and number counts of clusters of galaxies.

Acknowledgments

Partial financial support from NSF grants AST91-19216 and AST-95-00515, and from CNR-ASI grants are gratefully acknowledged. I wish to thank Florence, Daniel and Mme Raban for organizing a great meeting in always charming Paris.

References

1. G. Abell, *ApJS*, **3**, 211 (1958).
2. G. Abell *et al*, *ApJS*, **70**, 1 (1989).
3. R.H. Becker *et al*, *ApJ*, **450**, 559 (1995).
4. P.N. Best *et al*, *MNRAS*, **299**, 357 (1998).
5. D.C. Bock *et al*, *AJ*, **117**, 1578 (1999).
6. H. Böhringer *et al*, *The Messenger* **94**, 21 (1998).
7. H. Böhringer *et al*, astro-ph/0003219.
8. S. Borgani *et al*, these proceedings.
9. R.G. Bower *et al*, *MNRAS*, **281**, 59 (1996).
10. D.A. Bramel *et al*, astro-ph/9912275.
11. D.J. Burke *et al*, *ApJL*, **488**, L83 (1997).
12. S. Campana *et al*, *ApJ*, **524**, 423 (1999).
13. R.G. Carlberg *et al*, *ApJ*, **462**, 32 (1996).
14. K.C. Chambers *et al*, *ApJS*, **106**, 215 (1996).
15. K.C. Chambers *et al*, *ApJS*, **106**, 247 (1996).
16. D. Clowe *et al*, *ApJL*, **497**, L61 (1998).
17. D. Clowe *et al*, *ApJ*, **539**, 540 (2000).
18. C.A. Collins *et al*, *ApJL*, **479**, L117 (1997).

19. M. Colless, *Looking Deep in the Southern Sky*, eds. Morganti & Couch, 9 (1999).
20. M. Colless, *Clustering at high redshift*, ASP Conf. Series, eds. Mazure, LeFèvre, Le Brun, **200**, 3 (2000).
21. J.J. Condon *et al*, *AJ*, **115**, 1693 (1998).
22. W. Couch *et al*, *MNRAS*, **249**, 606 (1991).
23. C.S. Crawford & A.C. Fabian, *MNRAS*, **282**, 1483 (1996).
24. L.N. Da Costa, in *VLT Opening Symposium*, eds. J. Bergeron & A. Renzini, 192-197, (2000).
25. J. Dalcanton, *ApJ*, **466**, 92 (1996).
26. G.B. Dalton *et al*, *ApJ*, **390**, L1 (1992).
27. G.B. Dalton *et al*, *MNRAS*, **289**, 263 (1997).
28. R. Della Ceca *et al*, *A&A*, **353**, 498 (2000).
29. V. de Lapparent *et al*, *ApJ*, **302**, L1 (1986).
30. S. De Grandi *et al*, *ApJ*, **514**, 148 (1999).
31. M.E. Dickinson, *PH.D. Thesis*, University of California, Berkeley, 1994.
32. M.E. Dickinson, *HST and the High z Universe*, eds. Tavir, Aragon-Salamanca, & Wall, 207, (1997).
33. M.E. Donahue *et al*, *ApJ*, **497**, 573 (1998).
34. M.E. Donahue *et al*, *ApJ*, **527**, 525 (1999).
35. H. Ebeling & G. Wiedenmann *Phys. Rev. E* **47**, 704 (1993).
36. H. Ebeling *et al*, *MNRAS*, **301**, 881 (1998).
37. H. Ebeling *et al*, *MNRAS*, **318**, 333 (2000).
38. H. Ebeling *et al*, astro-ph/0009101.
39. H. Ebeling *et al*, *ApJ*, **534**, 133 (2000).
40. H. Ebeling *et al*, *Large Scale Structure in the X-ray Universe*", eds. Plionis & Georgantopoulos, 39-42, (2000).
41. C. Frenk *et al*, *ApJ*, **351**, 10 (1990).
42. I.M. Gioia *et al*, *ApJS*, **72**, 567 (1990).
43. I.M. Gioia *et al*, *ApJL*, **356**, L35 (1990).
44. I.M. Gioia & G.A. Luppino, *ApJS*, **94**, 583 (1994).
45. I.M. Gioia *et al*, *A&A*, **297**, L75 (1995).
46. I.M. Gioia *et al*, *AJ*, **117**, 2608 (1999).
47. I.M. Gioia, *Large Scale Structure in the X-ray Universe*", eds. Plionis & Georgantopoulos, 43-46, (2000).
48. I.M. Gioia, *Clustering at high redshifts*, eds. Mazure, LeFèvre, Le Brun, 221-225, (2000).
49. M.D. Gladders & H.K.C. Yee, astro-ph0004092.
50. J. Gunn *et al*, *ApJ*, **306**, 30 (1986).
51. L. Guzzo *et al*, *The Messenger* **95**, 27 (1999).
52. L. Guzzo *et al*, *Clustering at high redshift*, ASP Conf. Series, eds. Mazure, LeFèvre, Le Brun, **200**, 349 (2000).
53. J.P. Henry *et al*, *ApJ*, **368**, 408 (1992).
54. J.P. Henry *et al*, *ApJ*, **107**, 1270 (1994).
55. J.P. Henry *et al*, *AJ*, **114**, 1293 (1997).
56. G.J. Hill & S.J. Lilly, *ApJ*, **367**, 1 (1991).
57. B.P. Holden *et al*, *AJ*, **118**, 2002 (1999).
58. J.P. Huchra *et al*, *ApJS*, **52**, 89 (1982).
59. J.P. Huchra *et al*, *ApJS*, **121**, 287 (1999).
60. Jarret *et al*, *AJ*, , submitted (.)
61. L.R. Jones *et al*, *ApJ*, **495**, 100 (1997).
62. L.R. Jones *et al*, *Large Scale Structure in the X-ray Universe*", eds. Plionis & Georgantopoulos, 43-46, (2000).

- topoulos, 35-38, (2000).
63. W.C. Keel *et al*, *AJ*, **118**, 2547 (1999).
 64. J. Knapp *et al*, <http://www.astro.princeton.edu/PBOOK/welcome.htm>.
 65. J.D. Kurk *et al*, *A&A*, **358**, 1 (2000).
 66. D. Lazzati *et al*, *ApJ*, **524**, 414 (1999).
 67. O. LeFèvre *et al*, *ApJL*, **422**, L5 (1994).
 68. O. LeFèvre *et al*, *ApJ*, **471**, L11 (1996).
 69. O. LeFèvre, *Clustering at high redshift*, ASP Conf. Series, eds. Mazure, LeFèvre, Le Brun, **200**, 47 (2000).
 70. C. Lobo *et al*, *A&A*, **360**, 896 (2000).
 71. L.M. Lubin *et al*, *AJ*, **116**, 643 (1998).
 72. L.M. Lubin *et al*, *ApJ*, **531**, L5 (2000).
 73. S.L. Lumsden *et al*, *MNRAS*, **258**, 1 (1992).
 74. G.A. Luppino *et al*, *A&A Suppl. Ser.*, **136**, 117 (1999).
 75. G.A. Luppino & N. Kaiser, *ApJL*, **475**, 20 (1997).
 76. S. Maddox *et al*, *MNRAS*, **243**, 692 (1990).
 77. G.A. Mamon *et al*, *Wide Field Surveys in Cosmology*, eds. Colombi, Mellier, Raban, 323 (1998).
 78. B. Margon, *Phil. Trans. R. Soc. Lond. A*, **357**, 93 (1999).
 79. P.J. McCarthy *et al*, *ApJS*, **99**, 27 (1995).
 80. Y. Mellier, *Ann. Rev. A&A*, **37**, 127 (1999).
 81. C.R. Mullis *et al*, *The Hot Universe*, eds. Koyama, Kitamoto, Itoh, 473 (1998).
 82. C.R. Mullis, *Large Scale Structure in the X-ray Universe*", eds. Plionis & Georgantopoulos, 149-152, (2000).
 83. R.C. Nichol *et al*, *ApJL*, **521**, L21 (1999).
 84. J.B. Oke *et al*, *AJ*, **116**, 549 (1998).
 85. L.F. Olsen *et al*, *A&A*, **345**, 681 (1999a).
 86. L.F. Olsen *et al*, *A&A*, **345**, 363 (1999b).
 87. L.F. Olsen *et al*, *Clustering at high redshift*, eds. Mazure, LeFèvre, Le Brun, 440 (2000).
 88. S.M. Pascarelle *et al*, *ApJ*, **456**, L21 (1996).
 89. L. Pentericci *et al*, *A&A*, **326**, 580 (1997).
 90. L. Pentericci *et al*, *A&A*, **341**, 329 (1999).
 91. M. Postman *et al*, *AJ*, **111**, 615 (1996).
 92. M. Ramella *et al*, *A&A*, **360**, 861 (2000).
 93. R.B. Rengelink *et al*, *A&AS*, **124**, 259 (1997).
 94. A. Renzini & L.N. Da Costa, *The Messenger*, **87**, 23 (1997).
 95. A.K. Romer *et al*, *ApJS*, **126**, 209 (2000).
 96. P. Rosati *et al*, *ApJL*, **445**, L11 (1995).
 97. P. Rosati *et al*, *ApJL*, **492**, L21 (1998).
 98. P. Rosati *et al*, *AJ*, **118**, 76 (1999).
 99. P. Rosati *et al*, *Large Scale Structure in the X-ray Universe*", eds. Plionis & Georgantopoulos, 13-20, (2000).
 100. M. Rowan-Robinson *et al*, *MNRAS*, **247**, 1 (1990).
 101. W. Saunders *et al*, *Wide Field Surveys in Cosmology*, eds. Colombi, Mellier, Raban, 71 (1998).
 102. C. Scharf *et al*, *ApJ*, **477**, 79 (1997).
 103. C. Scharf *et al*, *ApJ*, **528**, 73 (2000).
 104. M. Scodreggio *et al*, *A&A*, **137**, 83 (1999).
 105. S.A. Shectman, *ApJ*, **179**, 681 (1973).
 106. S.A. Shectman, *ApJ*, **188**, 233 (1974).

107. S.A. Shectman, *ApJ*, **288**, 481 (1985).
108. S.A. Shectman *et al*, *ApJS*, **470**, 172 (1996).
109. G. Soucail *et al*, astro-ph/0006382.
110. S.A. Stanford *et al*, *A&A*, **114**, 2232 (1997).
111. J.T. Stocke *et al*, *ApJS*, **76**, 813 (1991).
112. J. Trümper, *Nature*, **349**, 579, (1991).
113. R.B. Tully, *ApJ*, **321**, 280 (1987).
114. M.P. Van Haarlem *et al*, *MNRAS*, **287**, 817 (1997).
115. V. Vikhlinin *et al*, *ApJ*, **502**, 558 (1998).
116. V. Vikhlinin *et al*, *ApJL*, **498**, L21 (1998).
117. V. Vikhlinin *et al*, *Large Scale Structure in the X-ray Universe*", eds. Plionis & Georgantopoulos, 31-34, (2000).
118. G. Vettolani *et al*, *A&A*, **32**, 954 (1997).
119. W. Voges *et al*, *A&A*, **349**, 389 (1999).
120. H.K.C. Yee *et al*, *ApJS*, **102**, 269 (1996).
121. H.K.C. Yee *et al*, *Highlights of Astronomy*, **11A**, 460, (1998).
122. D. Zaritsky *et al*, *ApJ*, **480**, L91 (1997).
123. F. Zwicky *et al*, *California Inst. Techn.*, (1968).